Applied Physics Letters

RESEARCH ARTICLE | OCTOBER 17 2024

(010) β-$(Al_x, Ga_{1-x})_2O_3$ growth using tritertiarybutylaluminum as Al gas precursor via hybrid molecular beam epitaxy

Zhuoqun Wen ; Xin Zhai ; Kamruzzaman Khan ; Oguz Odabasi ; Mijung Kim; Elaheh Ahmadi

Check for updates

Appl. Phys. Lett. 125, 162103 (2024)
https://doi.org/10.1063/5.0227366
CHORUS

View Online
Export Citation

Articles You May Be Interested In

Demonstration of mid-wavelength infrared nBn photodetectors based on type-II InAs/$InAs_{1-x}Sb_x$ superlattice grown by metal-organic chemical vapor deposition

Appl. Phys. Lett. (August 2019)

Lattice-matched epitaxial GaInAsSb/GaSb thermophotovoltaic devices

AIP Conference Proceedings (March 1997)

Si doping of β -Ga_2O_3 by disilane via hybrid plasma-assisted molecular beam epitaxy

Appl. Phys. Lett. (February 2023)

06 February 2025 21:51:12

AIP Publishing

Applied Physics Letters

Special Topics Open for Submissions

Learn More

AIP Publishing

Applied Physics Letters ARTICLE pubs.aip.org/aip/apl

(010) β-$(Al_x, Ga_{1-x})_2O_3$ growth using tritertiarybutylaluminum as Al gas precursor via hybrid molecular beam epitaxy

Cite as: Appl. Phys. Lett. **125**, 162103 (2024); doi: 10.1063/5.0227366
Submitted: 8 July 2024 · Accepted: 3 October 2024 ·
Published Online: 17 October 2024

View Online Export Citation CrossMark

Zhuoqun Wen,[1,a)] Xin Zhai,[2] Kamruzzaman Khan,[1] Oguz Odabasi,[3] Mijung Kim,[3] and Elaheh Ahmadi[3]

AFFILIATIONS

[1]Department of Materials Science and Engineering, University of Michigan, Ann Arbor, Michigan 48109, USA
[2]Department of Electrical Engineering and Computer Science, University of Michigan, Ann Arbor, Michigan 48109, USA
[3]Department of Electrical and Computer Engineering, University of California Los Angeles, California 90095, USA

[a)]Author to whom correspondence should be addressed: wzhuoqun@umich.edu

ABSTRACT

We report the epitaxial growth of (010) β-$(Al_xGa_{1-x})_2O_3$ using tritertiarybutylaluminum (TTBAl) as an aluminum gas precursor in a hybrid molecular beam epitaxy (h-MBE) system. In conventional MBE systems, a thermal effusion cell is typically used to supply Al. However, in an oxide MBE system, using a conventional Al effusion cell can cause difficulties due to the oxidation of the Al source during growth. This often requires breaking the vacuum frequently to reload Al. Our approach utilizes TTBAl, a gaseous Al source, via a h-MBE to circumvent the oxidation issues associated with traditional solid Al sources. We investigated the growth conditions of β-$(Al_xGa_{1-x})_2O_3$, varying TTBAl supply and growth temperature. For this purpose, we utilized both elemental Ga and Ga-suboxide as Ga precursors. Controllable and repeatable growth of β-$(Al_xGa_{1-x})_2O_3$ with Al compositions ranging from 1% to 25% was achieved. The impurity incorporation and crystal quality of the resulting β-$(Al_xGa_{1-x})_2O_3$ films were also studied. Using TTBAl as a gaseous precursor in h-MBE has proven to maintain stable Al supply, enabling the controlled growth of high-quality β-$(Al_xGa_{1-x})_2O_3$ films.

Published under an exclusive license by AIP Publishing. https://doi.org/10.1063/5.0227366

06 February 2025 21:51:12

β-Ga_2O_3 has emerged as a material of significant interest for the next generation high-power electronic applications and solar-blind ultraviolet (UV) detectors and as a substrate for UV light-emitting diodes (LEDs) due to its outstanding properties such as ultrawide bandgap ($E_g = 4.8$ eV) and the availability of producing low-cost, large-scale high-quality single crystal substrates.[1–10] β-Ga_2O_3-based power devices, including Schottky barrier diodes,[3,11–16] metal–semiconductor field-effect transistors (MESFETs),[17] and metal–oxide field-effect transistors (MOSFETs) with promising performance have already been demonstrated.[2,18–23]

Furthermore, considerable research has been conducted on epitaxial growth of β-$(Al_xGa_{1-x})_2O_3$ to enable design and fabrication of β-$(Al_xGa_{1-x})_2O_3$/β-Ga_2O_3 heterostructures. Such heterostructures pave the way for the development of advanced high-performance devices such as modulated doped field-effect transistors (MODFETs).[24–28] The interface of the β-$(Al_xGa_{1-x})_2O_3$/β-Ga_2O_3 heterostructure can enable carrier confinement, forming a two-dimensional electron gas (2DEG) with enhanced electron mobility.[29,30] Therefore, developing β-$(Al_xGa_{1-x})_2O_3$ epitaxial thin films is crucial.

The growth of β-$(Al_xGa_{1-x})_2O_3$ epitaxy with varying Al compositions has been reported using metal-organic chemical vapor deposition (MOCVD)[27,31–35] and molecular beam epitaxy (MBE) techniques.[36–39] However, the conventional oxide MBE system faces an oxidation challenge when employing solid sources for elements with high-melting-point oxides, such as Al.[40] The Al flux diminishes over time at a constant source temperature due to the formation of a solid Al_2O_3 layer on the Al surface. After each growth cycle, a higher source temperature is required to achieve the same Al flux, until eventually, the Al source is completely encapsulated by solid Al_2O_3, resulting in no flux. Various strategies have been employed to extend source life, including using a crucible with narrow orifice or inserting an endplate into the crucible.[41–43] Nonetheless, these methods only reduce the effects of source oxidation without completely resolving the issue.

Epitaxial growth of perovskites using conventional MBE has faced similar challenges due to oxidation of solid elemental sources and difficulties in controlling stoichiometry in ternary oxides due to suboxide desorption. Hybrid MBE, which integrates elemental and chemical gas sources, has been employed to address these

Published under an exclusive license by AIP Publishing

issues.[40,44–46] One significant breakthrough in this area was the use of titanium-tetraisopropoxide (TTIP) in conjunction with strontium for the growth of $SrTiO_3$.[47] This approach allowed for the self-regulated growth of high-quality films, demonstrating the potential of h-MBE for producing oxide materials with fewer defects and higher reproducibility. The success of h-MBE has since extended to other complex oxides, including rare earth titanates and vanadates,[48,49] providing a robust and adaptable method for material synthesis. Recently, we reported using diluted disilane as a silicon source for Si-doping of β-Ga_2O_3 to avoid challenges associated with the oxidation of solid silicon source.[50,51]

In this study, we propose the growth of β-$(Al_x, Ga_{1-x})_2O_3$ via h-MBE. To choose a proper metal-organic Al precursor, we considered two important properties: (i) vapor pressure and (ii) unintentional carbon incorporation due to metal-organic precursor. In particular, MBE system is an ultra-high vacuum (UHV) system, with the chamber pressure being approximately 10^{-10} Torr during the idle state and about 10^{-5} Torr during growth. Therefore, a gas precursor with relatively low vapor pressure is required to enable precise control of gas flow in the system. Common metal-organic Al gas precursors include trimethylaluminum (TMAl), triethylaluminum (TEAl), tritertiarybutylaluminum (TTBAl), aluminum-triisopropoxide (ATIP), and tri-n-octylaluminum (TNOAl). Among these precursors, TTBAl and TNOAl have relatively low vapor pressure at room temperature (~3 Torr for TTBAl and ~0.75 Torr for TNOAl). Since, compared to TNOAl, TTBAl has a lower carbon and hydrogen density, TTBAl was used as the Al precursor in our studies.

All samples were grown in a RIBER 32 hybrid MBE system equipped with conventional Ga, Ga-suboxide (Ga_2O), and Ge thermal effusion cells. The Ga_2O was made by mixing 99.999 99% (7 N) pure Ga with 99.999% (5 N) Ga_2O_3 powder, and a 5:2 molar ratio of Ga to Ga_2O_3 was added into the container and mixed in a heated water bath. The oxygen source consisted of ultra-high purified oxygen (> 99.999%) and was activated by the RIBER RF-O 50/63 oxygen RF plasma source. A plasma power and oxygen flow rate of 410 W and 2 sccm were used for all the growths discussed in this work. TTBAl is supplied through a specially designed gas delivery system. The TTBAl bubbler is placed in a container that is maintained at 0 °C by an ice–water mixture and is connected to a high-vacuum gas line. Upon opening, the TTBAl vapor enters the gas line, driven by the pressure differential. At 0 °C, the vapor pressure of TTBAl is 1.1 Torr. This vapor pressure is then regulated by an MKS 600 Series Pressure Controller, capable of maintaining and adjusting the vapor pressure within a 1 mTorr to 100 mTorr range. A flow restrictor, with different orifice diameters ranging from 100 μm to 3 mm, is utilized in this setup to further moderate the flow prior to its introduction into the ultra-high vacuum environment of the MBE chamber. The TTBAl vapor pressure delivered into the MBE chamber via a gas injector for the growth process is below 5×10^{-7} Torr, as measured by the ion gauge within the chamber. The gas injector is maintained at 60 °C during the growth to prevent the condensation of TTBAl gas. The Ga flux is measured by beam equivalent pressure (BEP) by the ion gauge. The schematic of our hybrid MBE system can be found in Ref. 50.

All epi-structures were grown on Sn-doped bulk (010) β-Ga_2O_3 substrates. Prior to the growth, 500 nm thick Ti layer was deposited on the backside of the substrates for better heat transfer as well as better adhesion to the silicon wafer via indium-bonding. The substrates were then diced into $5 \times 5\,mm^2$ or $5 \times 10\,mm^2$ pieces and after solvent-cleaning were indium-bonded to 3-in. Si wafers before being transferred into the growth chamber. The growth was initiated with 30 min of oxygen polishing (oxygen flow rate and RF power of 1 sccm and 350 W, respectively) followed by 30 min of Ga etching, using Ga BEP of 1×10^{-8} Torr, at 800 °C to remove impurities on the substrate surface.[6,28] Ga etching followed by O polishing can also help to remove the plasma damage related to O polishing.[28] Subsequently, $(Al,Ga)_2O_3$ films were grown in the h-MBE. For the secondary ion mass spectrometry (SIMS) stack, a 200 nm Ga_2O_3 unintentionally doped (UID) layer was first grown on the substrate to separate it from the SIMS layers.

The surface morphology and roughness of the grown layers were studied by atomic force microscopy (AFM). Secondary ion mass spectrometry (SIMS) was utilized to measure the Al composition and quantify unintentional incorporation of impurities such as hydrogen and carbon. High-resolution x-ray diffraction (HRXRD) and Rutherford backscattering spectrometry (RBS) analysis were used to determine the Al composition and layer thickness. The growth rate (GR) was then determined from the layer thickness measured by SIMS or XRD, knowing the duration of growth.

First, a series of samples were grown at 525 °C varying the TTBAl supply from BEP = 1.2×10^{-7} to 4.2×10^{-7} Torr while using a fixed Ga BEP of 1×10^{-8} Torr. The last sample was grown at TTBAl BEP = 4.2×10^{-7} Torr but with a Ga BEP of 5×10^{-9} Torr. The XRD ω–2θ triple-axis profiles were recorded along the (020) direction on these samples and are shown in Fig. 1. By changing TTBAl pressure from 1.2×10^{-7} to 4.2×10^{-7} Torr, β-$(Al_xGa_{1-x})_2O_3$ composition was changed from 1.8% to 14.9%, while the growth rate remained unchanged. For a maximum TTBAl pressure of 4.2×10^{-7} Torr, when Ga BEP was reduced to 5×10^{-9} Torr to further increase TTBAl/Ga ratio, β–γ phase segregation occurred, which has been widely observed on β-$(Al, Ga)_2O_3$ films grown by PAMBE with Al content higher than 15%.[7]

Next, a series of samples was grown using a TTBAl pressure of 4.3×10^{-7} Torr and a Ga BEP of 8×10^{-9} Torr, varying the substrate temperature (T_{sub}) from 525 to 725 °C. Figure 2 shows the AFM images taken on these samples along with the corresponding root mean square (rms) surface roughness. The sample grown at T_{sub} = 525 °C exhibited a relatively rough surface with the presence of

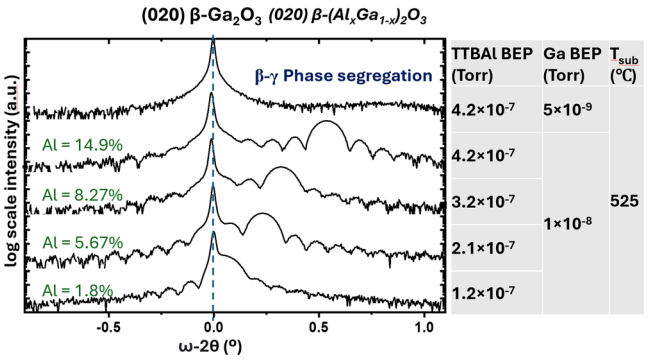

FIG. 1. HRXRD of (010) β-$(Al_xGa_{1-x})_2O_3$ grown using TTBAl, Ga, and O plasma in h-MBE system at substrate temperature = 525 °C. Al composition ranges from 1.8% to 14.9% with different TTBAl/Ga ratios at T_{sub} = 525 °C. β–γ phase segregation is observed when the TTBAl/Ga ratio is further increased at T_{sub} = 525 °C.

06 February 2025 21:51:12

Published under an exclusive license by AIP Publishing

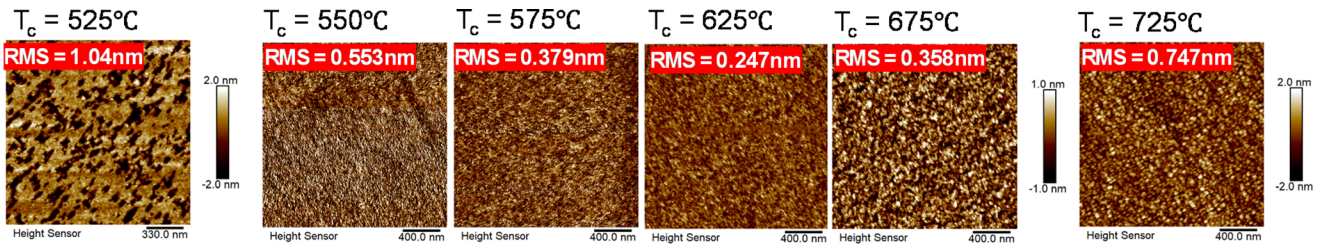

FIG. 2. AFM of β-$(Al_xGa_{1-x})_2O_3$ at different T_{sub}. TTBAl pressure $= 4.3 \times 10^{-7}$ Torr; Ga BEP $= 8 \times 10^{-9}$ Torr were used during all the growths here.

pinholes. During growth, Al, Ga, and O atoms move across the substrate surface, requiring energy to bond into the final AlGaO compound. At lower temperatures, the energy provided to the substrate may be insufficient to allow adequate adatom mobility for the Al atoms, which can lead to pinholes on the surface. As the growth temperature increased, the surface roughness initially decreased, reaching a minimum rms of 0.247 nm at 625 °C before subsequently increasing again.

Figure 3 shows the HRXRD profile of the grown samples using Ga and Ga-suboxide as Ga precursor. Our previous studies showed that replacing the Ga source with Ga_2O almost doubled the maximum GR of Ga_2O_3.[51] Ga_2O was produced by mixing 7 N pure Ga with 5 N Ga_2O_3 powder in a 5:2 molar ratio of Ga to Ga_2O_3. A set of samples was grown using Ga_2O BEP of 1×10^{-7} Torr and TTBAl pressure of 4.3×10^{-7} Torr, with the growth temperature varying from 525 °C to 725 °C. Table I summarizes T_{sub}, Al composition, and GR for each sample.

From Fig. 3(a), the samples grown by Ga source at temperatures ranging from $T_{sub} = 525$ to 575 °C, the composition and GR remained approximately constant. As the temperature increased further, the GR of β-(Al, Ga)$_2O_3$ decreased and the Al composition increased accordingly. The lower growth rate at higher temperatures is due to the formation and thermal desorption of volatile Ga_2O.[52] The Al composition reached 25.4% at $T_{sub} = 675$ °C, with a GR of 40 nm/h. Growth ceased when T_{sub} reached 725 °C due to the high desorption of Ga_2O at high growth temperatures.

As shown in Fig. 3(b), similar to the samples grown by Ga source, the Al composition and GR remained the same at 200 nm/h from $T_{sub} = 525$ to 575 °C using Ga-suboxide as precursor, with Al composition around 6.3%–7.2%. The growth rate doubled compared to the GR measured on samples grown using the Ga source, which consequently halved the Al composition. No thickness fringes were observed in the XRD profile of the sample grown at $T_{sub} = 525$ °C, indicating relatively poor quality at this temperature. As the growth temperature increased further, the GR dropped, and Al composition increased. It is worth noting that, as discussed earlier, no epitaxial growth occurred at $T_{sub} = 725$ °C using the Ga source, whereas $(Al_xGa_{1-x})_2O_3$ films with a GR of 51 nm/h and an Al composition of 16.3% were achieved using the Ga_2O source. This may be attributed to the increased partial pressure of Ga_2O in the chamber when Ga_2O is used as the Ga precursor, which leads to a shift in thermal equilibrium favoring the formation of Ga_2O_3 from desorption. This equilibrium shift results in the growth of $(Al_xGa_{1-x})_2O_3$ even at the high temperature of 725 °C, where desorption would typically prevent epitaxial growth using the Ga source.

TABLE I. Summary of β-$(Al_xGa_{1-x})_2O_3$ samples grown by Ga and Ga-suboxide at different growth temperatures. The Al% and GR are extracted from HRXRD presented in Fig. 3.

Precursor	Ga		Ga-suboxide	
T_{sub} (°C)	GR (nm/h)	Al (%)	GR (nm/h)	Al (%)
725	Null	Null	51	16.3
675	40	25.4	83	11.8
625	60	21.8	113	8.9
575	86	14.2	200	6.9
550	84	14.9	200	6.3
525	83	14.9	200	7.2

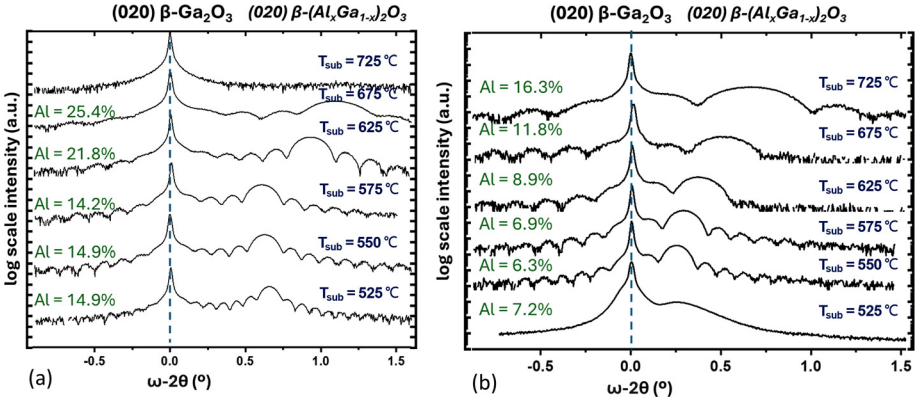

FIG. 3. (a) HRXRD of β-$(Al_xGa_{1-x})_2O_3$ in h-MBE system at different T_{sub}. TTBAl $= 4.3 \times 10^{-7}$ Torr; Ga BEP $= 8 \times 10^{-9}$ Torr were used during all the growths. (b) HRXRD of β-$(Al_xGa_{1-x})_2O_3$ grown by Ga-suboxide at different T_{sub}. TTBAl $= 4.3 \times 10^{-7}$ Torr; Ga-suboxide BEP $= 1 \times 10^{-7}$ Torr were used during all the growth processes.

06 February 2025 21:51:12

Published under an exclusive license by AIP Publishing

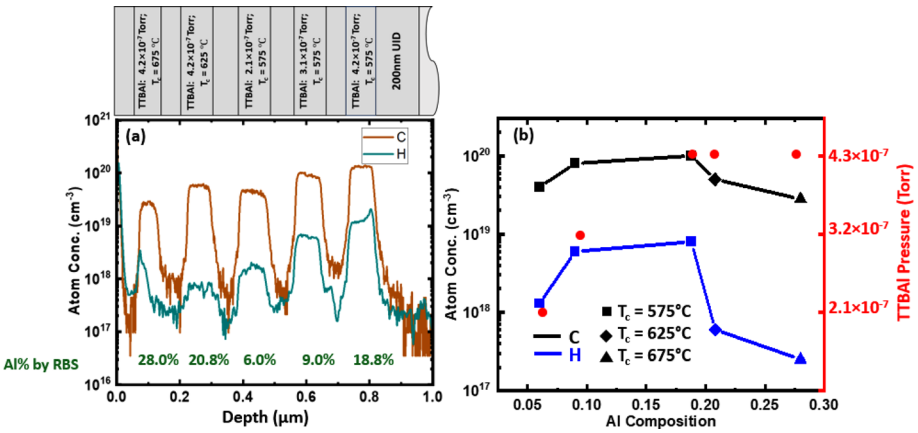

FIG. 4. (a) SIMS analysis of C and H concentrations in (010) β-(Al, Ga)$_2$O$_3$ growth by TTBAl and Ga. (b) Average C and H concentrations vs Al composition at each layer.

To analyze unintentionally incorporated impurities in (Al, Ga)$_2$O$_3$ films, a SIMS stack was grown with the epi-structure shown in Fig. 4. In this sample, a 200 nm thick layer of unintentionally doped (UID) Ga_2O_3 was grown to isolate (Al, Ga)$_2$O$_3$ layers from the substrate. Subsequently, each (Al, Ga)$_2$O$_3$ layer was grown over a period of 2 h, with variations TTBAl pressures or growth temperatures, separated by 100 nm of UID Ga_2O_3. The SIMS analysis was conducted by EAG Laboratories. However, reliable calibrations for Al content in $(Al_xGa_{1-x})_2O_3$ (where $1 < x < 30$) have yet to be demonstrated. To achieve more accurate Al composition, RBS analysis was performed on these samples instead. The Al compositions determined by RBS were in good agreement with the results obtained from XRD measurements. The Al composition for each layer of the SIMS stack was characterized by RBS. The RBS spectra of the sample are shown in the supplementary material. The results are presented in Fig. 4(b). At $T_{sub} = 575\,^{\circ}C$, increasing the TTBAl supply from 2.1×10^{-7} to 4.3×10^{-7} Torr resulted in an increase in Al composition from 6.0% to 18.8%. Simultaneously, the concentrations of impurities such as C and H, likely originating from TTBAl, increased from 4×10^{19} to $1 \times 10^{20}\,cm^{-3}$ and from 1.3×10^{18} to $8 \times 10^{18}\,cm^{-3}$, respectively. In the final two layers, where T_{sub} was increased to 625 and 675 °C while maintaining the TTBAl at 4.3×10^{-7} Torr, the Al composition continued to increase and the GR decreased, corroborating previous XRD results. Interestingly, at these higher temperatures, both C and H densities decreased. C density dropped from 1×10^{20} to $2.8 \times 10^{19}\,cm^{-3}$, and H density decreased from 8×10^{18} to $2.5 \times 10^{17}\,cm^{-3}$. While a C incorporation of $2.8 \times 10^{19}\,cm^{-3}$ is still considered high, H incorporation reached levels nearly identical to those of the substrate. However, a significant decrease in the growth rate was observed with increasing T_{sub}, and no epitaxial growth occurred at $T_{sub} = 725\,^{\circ}C$. The incorporation of carbon and hydrogen is influenced by the substrate temperature, indicating that the reaction mechanism (including the bonding and debonding processes) of TTBAl during growth is temperature dependent. Further analysis is needed to fully understand this mechanism and to reduce the C and H impurities in the grown thin film. Investigating alternative gas sources for Al may be beneficial in future studies.

In summary, we demonstrated the growth of β-$(Al_xGa_{1-x})_2O_3$ using TTBAl as a gaseous aluminum source in h-MBE, which presents a promising solution for overcoming the traditional challenges of Al source oxidation in oxide MBE. Our studies show that β-$(Al_xGa_{1-x})_2O_3$ compositions can be controlled from 1% to 25% by adjusting the TTBAl pressure and substrate temperature. Additionally, we showed that growth at higher temperatures can reduce the incorporation of impurities such as carbon and hydrogen. This growth technique not only provides a repeatable and controllable method for growing β-$(Al_xGa_{1-x})_2O_3$ films with varying Al composition but also extends the potential for future research into other complex oxide materials using h-MBE systems.

See the supplementary material for the RBS results are shown in Fig. S1. Both RBS and SIMS analysis were done by Eurofins EAG Laboratories.

This work was supported by the Air Force Office of Scientific Research (Program Manager, Dr Ali Sayir) through Program FA9550-20-1-0045, the National Science Foundation under Grant Nos. 2043803 and 2244040, and DARPA under Grant No. N660012214032.

AUTHOR DECLARATIONS

Conflict of Interest

The authors have no conflicts to disclose.

Author Contributions

Zhuoqun Wen: Conceptualization (equal); Data curation (equal); Formal analysis (lead); Investigation (lead); Methodology (lead); Validation (lead); Visualization (lead); Writing – original draft (lead); Writing – review & editing (equal). **Xin Zhai:** Formal analysis (equal); Investigation (equal); Methodology (equal); Validation (equal); Writing – review & editing (equal). **Kamruzzaman Khan:** Investigation (equal); Methodology (equal); Writing – review & editing (equal). **Oguz Odabasi:** Formal analysis (equal); Methodology (equal); Visualization (equal); Writing – review & editing (equal). **Mijung Kim:** Data curation (equal); Investigation (equal); Writing – review & editing (equal). **Elaheh Ahmadi:** Conceptualization (equal); Data curation (equal); Formal analysis (equal); Funding acquisition (lead); Investigation (equal); Methodology (equal); Supervision (lead); Validation (equal); Visualization (equal); Writing – original draft (equal); Writing – review & editing (equal).

06 February 2025 21:51:12

Published under an exclusive license by AIP Publishing

DATA AVAILABILITY

The data that support the findings of this study are available from the corresponding author upon reasonable request.

REFERENCES

[1]J. Zhang, J. Shi, D.-C. Qi, L. Chen, and K. H. Zhang, "Recent progress on the electronic structure, defect, and doping properties of Ga_2O_3," APL Mater. **8**(2), 020906 (2020).

[2]S. Pearton, F. Ren, M. Tadjer, and J. Kim, "Perspective: Ga_2O_3 for ultra-high power rectifiers and MOSFETS," J. Appl. Phys. **124**(22), 220901 (2018).

[3]L. Du, Q. Xin, M. Xu, Y. Liu, W. Mu, S. Yan, X. Wang, G. Xin, Z. Jia, and X.-T. Tao, "High-performance Ga_2O_3 diode based on tin oxide Schottky contact," IEEE Electron Device Lett. **40**(3), 451–454 (2019).

[4]M. A. Bhuiyan, H. Zhou, R. Jiang, E. X. Zhang, D. M. Fleetwood, D. Y. Peide, and T.-P. Ma, "Charge trapping in Al_2O_3/β-Ga_2O_3-based MOS capacitors," IEEE Electron Device Lett. **39**(7), 1022–1025 (2018).

[5]E. Ahmadi, O. S. Koksaldi, S. W. Kaun, Y. Oshima, D. B. Short, U. K. Mishra, and J. S. Speck, "Ge doping of β-Ga_2O_3 films grown by plasma-assisted molecular beam epitaxy," Appl. Phys. Express **10**(4), 041102 (2017).

[6]Y. Oshima, E. Ahmadi, S. Kaun, F. Wu, and J. S. Speck, "Growth and etching characteristics of (001) β-Ga_2O_3 by plasma-assisted molecular beam epitaxy," Semicond. Sci. Technol. **33**(1), 015013 (2017).

[7]S. W. Kaun, F. Wu, and J. S. Speck, "β-$(Al_xGa_{1-x})_2O_3/Ga_2O_3$ (010) heterostructures grown on β-Ga_2O_3 (010) substrates by plasma-assisted molecular beam epitaxy," J. Vac. Sci. Technol., A **33**(4), 041508 (2015).

[8]X. Zhai, Z. Wen, O. Odabasi, E. Achamyeleh, K. Sun, and E. Ahmadi, "Investigation of ALD $HfSiO_x$ as gate dielectric on β-Ga_2O_3 (001)," Appl. Phys. Lett. **124**(13), 132103 (2024).

[9]Z. Wen, K. Khan, K. Sun, R. Wellen, Y. Oshima, and E. Ahmadi, "Thermal stability of HVPE-grown (0001) α-Ga_2O_3 on sapphire template under vacuum and atmospheric environments," J. Vac. Sci. Technol., A **41**(4), 043403 (2023).

[10]X. Xia, J.-S. Li, Z. Wen, K. Khan, M. I. Khan, E. Ahmadi, Y. Oshima, D. C. Hays, F. Ren, and S. Pearton, "Type-II band alignment for atomic layer deposited $HfSiO_4$ on α-Ga_2O_3," J. Vac. Sci. Technol., A **41**(2), 023205 (2023).

[11]L. Du, Q. Xin, M. Xu, Y. Liu, G. Liang, W. Mu, Z. Jia, X. Wang, G. Xin, and X.-T. Tao, "Achieving high performance Ga_2O_3 diodes by adjusting chemical composition of tin oxide Schottky electrode," Semicond. Sci. Technol. **34**(7), 075001 (2019).

[12]M. Higashiwaki, K. Konishi, K. Sasaki, K. Goto, K. Nomura, Q. T. Thieu, R. Togashi, H. Murakami, Y. Kumagai, and B. Monemar, "Temperature-dependent capacitance–voltage and current–voltage characteristics of Pt/Ga_2O_3 (001) Schottky barrier diodes fabricated on n^-–Ga_2O_3 drift layers grown by halide vapor phase epitaxy," Appl. Phys. Lett. **108**(13), 133503 (2016).

[13]C. Joishi, S. Rafique, Z. Xia, L. Han, S. Krishnamoorthy, Y. Zhang, S. Lodha, H. Zhao, and S. Rajan, "Low-pressure CVD-grown β-Ga_2O_3 bevel-field-plated Schottky barrier diodes," Appl. Phys. Express **11**(3), 031101 (2018).

[14]K. Konishi, K. Goto, H. Murakami, Y. Kumagai, A. Kuramata, S. Yamakoshi, and M. Higashiwaki, "1-kV vertical Ga_2O_3 field-plated Schottky barrier diodes," Appl. Phys. Lett. **110**(10), 103506 (2017).

[15]T. Oishi, Y. Koga, K. Harada, and M. Kasu, "High-mobility β-Ga_2O_3 ($\bar{2}$01) single crystals grown by edge-defined film-fed growth method and their Schottky barrier diodes with Ni contact," Appl. Phys. Express **8**(3), 031101 (2015).

[16]R. Suzuki, S. Nakagomi, Y. Kokubun, N. Arai, and S. Ohira, "Enhancement of responsivity in solar-blind β-Ga_2O_3 photodiodes with a Au Schottky contact fabricated on single crystal substrates by annealing," Appl. Phys. Lett. **94**(22), 222102 (2009).

[17]J. F. McGlone, Z. Xia, Y. Zhang, C. Joishi, S. Lodha, S. Rajan, S. A. Ringel, and A. R. Arehart, "Trapping effects in Si δ-doped β-Ga_2O_3 MESFETs on an Fe-doped β-Ga_2O_3 substrate," IEEE Electron Device Lett. **39**(7), 1042–1045 (2018).

[18]M. H. Wong, K. Goto, Y. Morikawa, A. Kuramata, S. Yamakoshi, H. Murakami, Y. Kumagai, and M. Higashiwaki, "All-ion-implanted planar-gate current aperture vertical Ga_2O_3 MOSFETs with Mg-doped blocking layer," Appl. Phys. Express **11**(6), 064102 (2018).

[19]M. H. Wong, K. Goto, H. Murakami, Y. Kumagai, and M. Higashiwaki, "Current aperture vertical β-Ga_2O_3 MOSFETs fabricated by N-and Si-ion implantation doping," IEEE Electron Device Lett. **40**(3), 431–434 (2019).

[20]M. H. Wong, H. Murakami, Y. Kumagai, and M. Higashiwaki, "Enhancement-mode β-Ga_2O_3 current aperture vertical MOSFETs with N-ion-implanted blocker," IEEE Electron Device Lett. **41**(2), 296–299 (2020).

[21]M. H. Wong, K. Sasaki, A. Kuramata, S. Yamakoshi, and M. Higashiwaki, "Field-plated Ga_2O_3 MOSFETs with a breakdown voltage of over 750 V," IEEE Electron Device Lett. **37**(2), 212–215 (2016).

[22]M. H. Wong, K. Sasaki, A. Kuramata, S. Yamakoshi, and M. Higashiwaki, "Electron channel mobility in silicon-doped Ga_2O_3 MOSFETs with a resistive buffer layer," Jpn. J. Appl. Phys., Part 1 **55**(12), 1202B9 (2016).

[23]N. Moser, J. McCandless, A. Crespo, K. Leedy, A. Green, A. Neal, S. Mou, E. Ahmadi, J. Speck, and K. Chabak, "Ge-doped β-Ga_2O_3 MOSFETs," IEEE Electron Device Lett. **38**(6), 775–778 (2017).

[24]A. D. Meshram, A. Sengupta, T. K. Bhattacharyya, and G. Dutta, "Normally-off β-$(Al_xGa_{1-x})_2O_3/Ga_2O_3$ modulation-doped field-effect transistors with p-GaN gate: Proposal and investigation," IEEE Trans. Electron Devices **70**(2), 454–460 (2023).

[25]X. Jia, Y. Wang, C. Fang, B. Li, Z. Luo, Y. Liu, Y. Hao, and G. Han, "Characteristics of β-$(Al_xGa_{1-x})_2O_3/Ga_2O_3$ dual-metal gate modulation-doped field-effect transistors simulated by TCAD," J. Vac. Sci. Technol., B **42**(3), 032207 (2024).

[26]A. D. Meshram, A. Sengupta, T. K. Bhattacharyya, and G. Dutta, "ON-and OFF-state performance of normally-OFF β-$(Al_xGa_{1-x})_2O_3/Ga_2O_3$ MODFETs with p-GaN gate," in *IEEE 20th India Council International Conference (INDICON)* (IEEE, 2023), pp. 673–678.

[27]F. Alema, T. Itoh, W. Brand, M. Tadjer, A. Osinsky, and J. S. Speck, "N_2O grown high Al composition nitrogen doped β-$(AlGa)_2O_3/\beta$-Ga_2O_3 using MOCVD," J. Vac. Sci. Technol., A **41**(4), 042709 (2023).

[28]E. Ahmadi, O. S. Koksaldi, X. Zheng, T. Mates, Y. Oshima, U. K. Mishra, and J. S. Speck, "Demonstration of β-$(Al_xGa_{1-x})_2O_3/\beta$-$Ga_2O_3$ modulation doped field-effect transistors with Ge as dopant grown via plasma-assisted molecular beam epitaxy," Appl. Phys. Express **10**(7), 071101 (2017).

[29]Y. Zhang, Z. Xia, J. Mcglone, W. Sun, C. Joishi, A. R. Arehart, S. A. Ringel, and S. Rajan, "Evaluation of low-temperature saturation velocity in β-$(Al_xGa_{1-x})_2O_3/Ga_2O_3$ modulation-doped field-effect transistors," IEEE Trans. Electron Devices **66**(3), 1574–1578 (2019).

[30]N. K. Kalarickal, Z. Xia, J. F. McGlone, Y. Liu, W. Moore, A. R. Arehart, S. A. Ringel, and S. Rajan, "High electron density β-$(Al_{0.17}Ga_{0.83})_2O_3/Ga_2O_3$ modulation doping using an ultra-thin (1 nm) spacer layer," J. Appl. Phys. **127**(21), 215706 (2020).

[31]A. Bhuiyan, Z. Feng, J. M. Johnson, H.-L. Huang, J. Hwang, and H. Zhao, "Band offsets of (100) β-$(Al_xGa_{1-x})_2O_3/\beta$-$Ga_2O_3$ heterointerfaces grown via MOCVD," Appl. Phys. Lett. **117**(25), 252105 (2020).

[32]A. Bhuiyan, Z. Feng, J. M. Johnson, H.-L. Huang, J. Hwang, and H. Zhao, "MOCVD growth of β-phase $(Al_xGa_{1-x})_2O_3$ on ($\bar{2}$01) β-Ga_2O_3 substrates," Appl. Phys. Lett. **117**(14), 142107 (2020).

[33]A. Anhar Uddin Bhuiyan, Z. Feng, J. M. Johnson, Z. Chen, H.-L. Huang, J. Hwang, and H. Zhao, "MOCVD epitaxy of β-$(Al_xGa_{1-x})_2O_3$ thin films on (010) Ga_2O_3 substrates and N-type doping," Appl. Phys. Lett. **115**(12), 120602 (2019).

[34]P. Ranga, A. Bhattacharyya, A. Chmielewski, S. Roy, R. Sun, M. A. Scarpulla, N. Alem, and S. Krishnamoorthy, "Growth and characterization of metalorganic vapor-phase epitaxy-grown β-$(Al_xGa_{1-x})_2O_3/\beta$-$Ga_2O_3$ heterostructure channels," Appl. Phys. Express **14**(2), 025501 (2021).

[35]R. Miller, F. Alema, and A. Osinsky, "Epitaxial β-Ga_2O_3 and β-$(Al_xGa_{1-x})_2O_3/\beta$-$Ga_2O_3$ heterostructures growth for power electronics," IEEE Trans. Semicond. Manuf. **31**(4), 467–474 (2018).

[36]Y. Zhang, A. Mauze, and J. S. Speck, *Development of β-(AlxGa1-x)2O3/Ga2O3 Heterostructures* (University of California, Santa Barbara, 2019).

[37]A. Jian, K. Khan, and E. Ahmadi, "β-(Al, Ga)$_2O_3$ for high power applications—A review on material growth and device fabrication," Int. J. High Speed Electron. Syst. **28**(01n02), 1940006 (2019).

[38]Y. Oshima, E. Ahmadi, S. C. Badescu, F. Wu, and J. S. Speck, "Composition determination of β-$(Al_xGa_{1-x})_2O_3$ layers coherently grown on (010) β-Ga_2O_3 substrates by high-resolution x-ray diffraction," Appl. Phys. Express **9**(6), 061102 (2016).

[39]E. Ahmadi, Y. Oshima, F. Wu, and J. S. Speck, "Schottky barrier height of Ni to β-$(Al_xGa_{1-x})_2O_3$ with different compositions grown by plasma-assisted molecular beam epitaxy," Semicond. Sci. Technol. **32**(3), 035004 (2017).

06 February 2025 21:51:12

Published under an exclusive license by AIP Publishing

[40]M. Brahlek, A. S. Gupta, J. Lapano, J. Roth, H. T. Zhang, L. Zhang, R. Haislmaier, and R. Engel-Herbert, "Frontiers in the growth of complex oxide thin films: Past, present, and future of hybrid MBE," Adv. Funct. Mater. **28**(9), 1702772 (2018).
[41]W. Nunn, T. K. Truttmann, and B. Jalan, "A review of molecular-beam epitaxy of wide bandgap complex oxide semiconductors," J. Mater. Res. **36**, 4846–4864 (2021).
[42]Y.-S. Kim, N. Bansal, and S. Oh, "Crucible aperture: An effective way to reduce source oxidation in oxide molecular beam epitaxy process," J. Vac. Sci. Technol., A **28**(4), 600–602 (2010).
[43]J. McCandless, V. Protasenko, B. Morell, E. Steinbrunner, A. Neal, N. Tanen, Y. Cho, T. Asel, S. Mou, and P. Vogt, "Controlled Si doping of β-Ga_2O_3 by molecular beam epitaxy," Appl. Phys. Lett. **121**(7), 072108 (2022).
[44]B. Fazlioglu-Yalcin, A. C. Suceava, T. Kuznetsova, K. Wang, V. Gopalan, and R. Engel-Herbert, "Stoichiometric control and optical properties of $BaTiO_3$ thin films grown by hybrid MBE," Adv. Mater. Inter. **10**(11), 2300018 (2023).
[45]M. Brahlek, L. Zhang, H.-T. Zhang, J. Lapano, L. R. Dedon, L. W. Martin, and R. Engel-Herbert, "Mapping growth windows in quaternary perovskite oxide systems by hybrid molecular beam epitaxy," Appl. Phys. Lett. **109**(10), 101903 (2016).
[46]A. Prakash, J. Dewey, H. Yun, J. S. Jeong, K. A. Mkhoyan, and B. Jalan, "Hybrid molecular beam epitaxy for the growth of stoichiometric $BaSnO_3$," J. Vac. Sci. Technol., A **33**(6), 060608 (2015).
[47]B. Jalan, P. Moetakef, and S. Stemmer, "Molecular beam epitaxy of $SrTiO_3$ with a growth window," Appl. Phys. Lett. **95**(3), 032906 (2009).
[48]X. Gu, "High quality molecular beam epitaxy growth and characterization of lead titanate zirconate based complex-oxides," Ph.D. dissertation (Virginia Commonwealth University, 2007).
[49]J. A. Moyer, C. Eaton, and R. Engel-Herbert, "Highly conductive $SrVO_3$ as a bottom electrode for functional perovskite oxides," Adv. Mater. **25**(26), 3578–3582 (2013).
[50]Z. Wen, K. Khan, X. Zhai, and E. Ahmadi, "Si doping of β-Ga_2O_3 by disilane via hybrid plasma-assisted molecular beam epitaxy," Appl. Phys. Lett. **122**(8), 082101 (2023).
[51]Z. Wen, X. Zhai, C. Lee, S. Kosanovic, Y. Kim, A. T. Neal, T. Asel, S. Mou, and E. Ahmadi, "Investigation of Si incorporation in (010) β-Ga_2O_3 films grown by plasma-assisted MBE using diluted disilane as Si source and suboxide Ga_2O precursor," Appl. Phys. Lett. **124**(12), 122101 (2024).
[52]P. Vogt and O. Bierwagen, "Reaction kinetics and growth window for plasma-assisted molecular beam epitaxy of Ga_2O_3: Incorporation of Ga vs. Ga_2O desorption," Appl. Phys. Lett. **108**(7), 072101 (2016).

06 February 2025 21:51:12

Published under an exclusive license by AIP Publishing